
Figures and figure supplements

Cortical motor activity modulates respiration and reduces apnoea in neonates

Coen S Zandvoort et al.

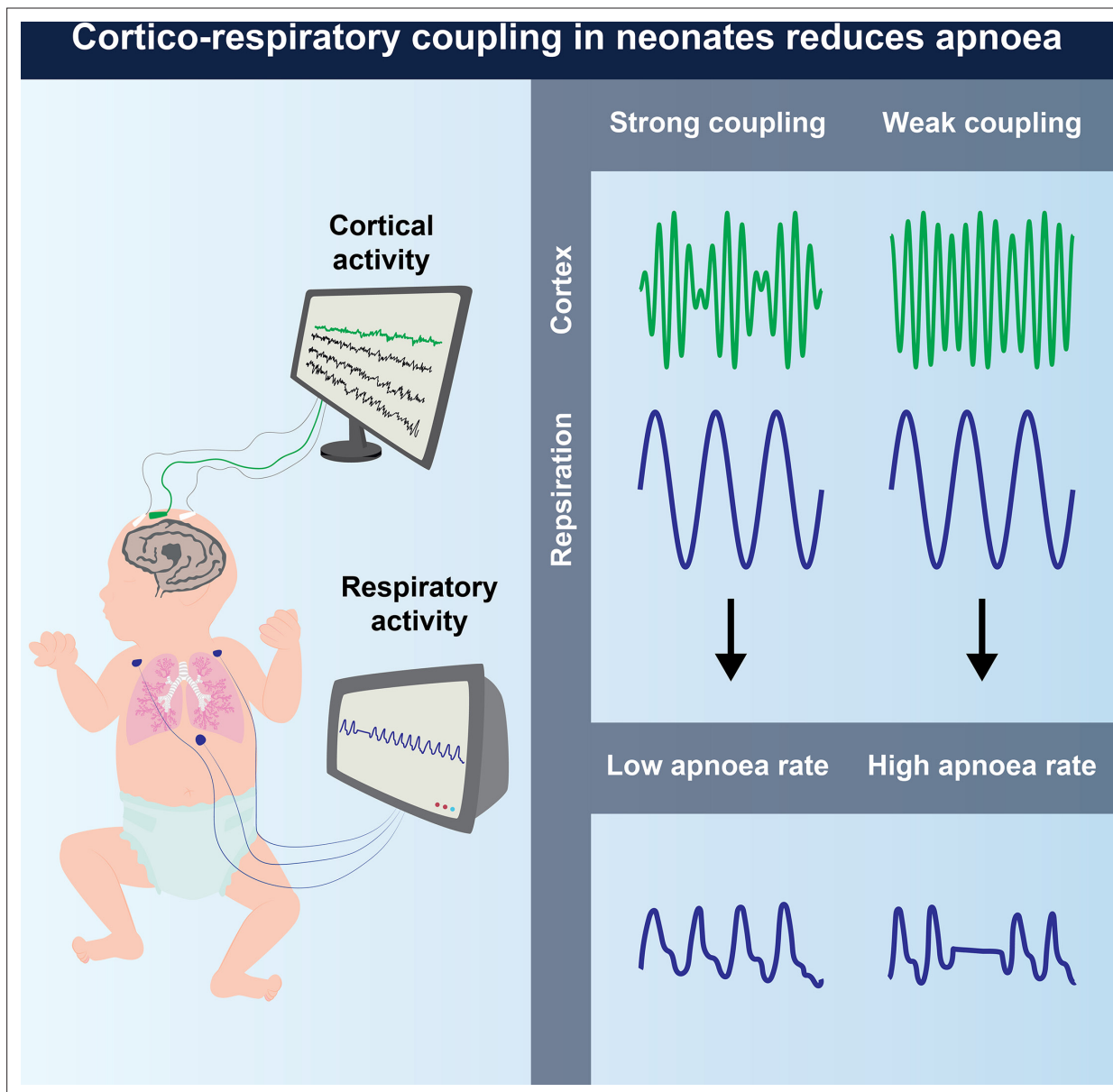


Figure 1. Schematic of the data acquisition setup (left panel) and main findings (right panel). Each recording consisted of cortical activity (using electroencephalography) and respiratory activity (using impedance pneumography).

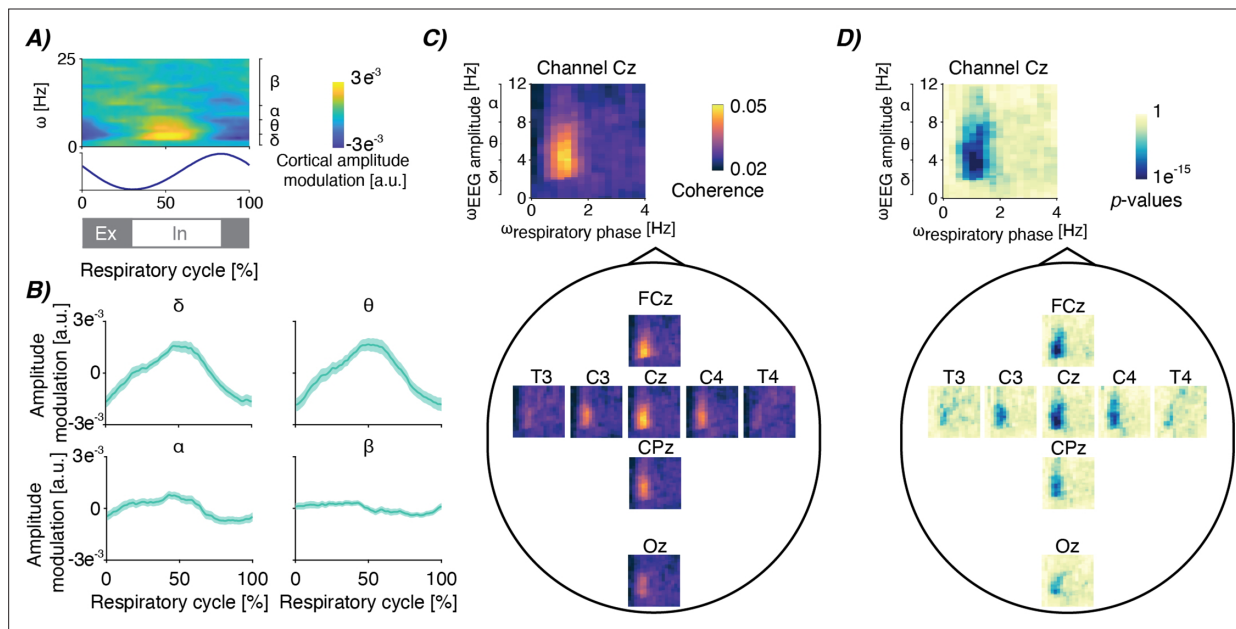


Figure 2. Cortico-respiratory coupling in infants. **(A)** Electroencephalographic (EEG) amplitude modulation depending on the respiratory cycle and frequency. EEG amplitude is averaged over breaths, recordings and channels FCz and Cz. The blue graph below is the impedance pneumographic signal time-locked from breath to breath and averaged over breaths and recordings. Grey and white bars below indicate expiration (Ex; in grey) and inspiration (In; in white). **(B)** The time-resolved amplitude modulations averaged within four frequency bands (delta: 0.5–4 Hz, theta: 4–8 Hz, alpha: 8–13 Hz, beta: 13–25 Hz), focusing on channels FCz and Cz again. Shaded light-green area is the standard error across recordings after pooling over channels. **(C)** Spatial map of coherence-based phase-amplitude coupling (PAC) between the respiratory phase ($\omega_{\text{respiratory phase}}$) and EEG amplitude ($\omega_{\text{EEG amplitude}}$) – see **Figure 2—figure supplement 1** for the pan-spectral PAC estimates. Spectra are the mean over all recordings. **(D)** Spatial map for the corresponding (uncorrected) statistical significance relative to surrogate PAC obtained through epoch shuffling (reported on a logarithmic scale). For all panels, data included is from 68 infants (28–42 weeks postmenstrual age [PMA] at time of recording) on 104 recording occasions. See **Table 1** for further clinical and demographic characteristics.

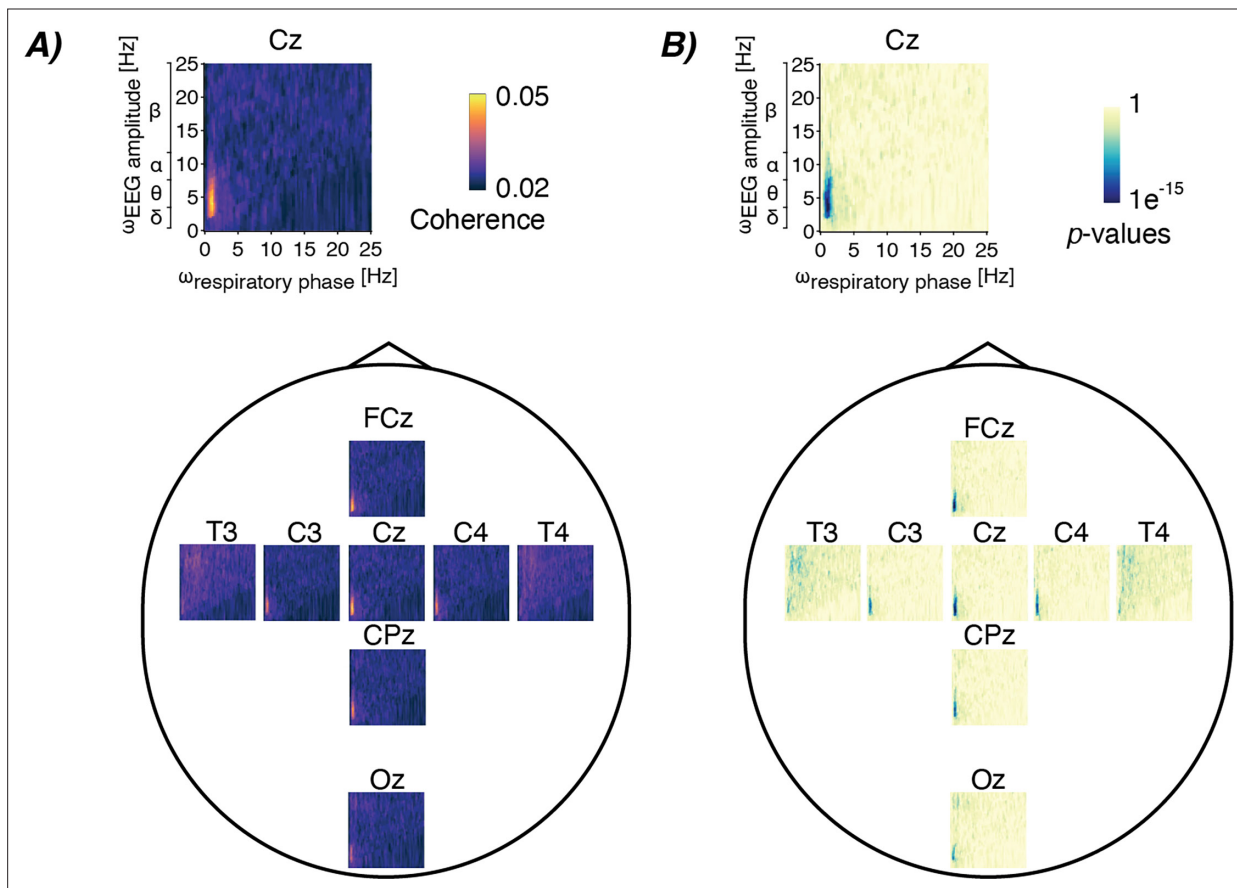


Figure 2—figure supplement 1. Cortico-respiratory coupling in infants. (A) Spatial map of coherence-based phase-amplitude coupling (PAC) between respiratory phase ($\omega_{\text{respiratory phase}}$) and electroencephalography (EEG) amplitude ($\omega_{\text{EEG amplitude}}$) over full frequency ranges (**Figure 2** depicts the zoomed-in spectra). (B) Analogous spatial map for the (uncorrected) statistical significance relative to surrogate PAC (reported on a logarithmic scale).

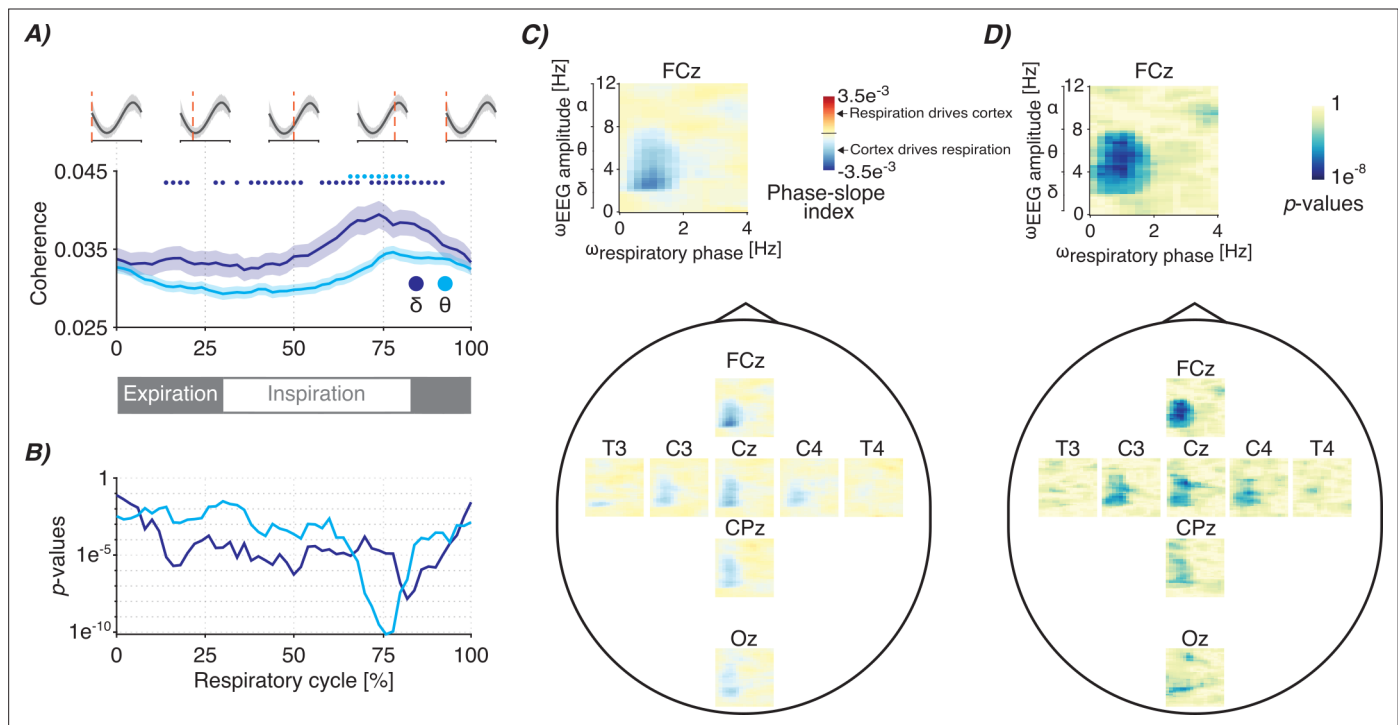


Figure 3. Timing and directionality of the cortico-respiratory coupling. **(A)** Phase-amplitude coupling (PAC) modulation (estimated as cross-frequency coherence) throughout the respiratory cycle. Graphs are colour-coded for the delta- and theta-frequency bands (dark- and light-blue colours, respectively), which are the electroencephalography (EEG's) primary frequency bands for which we observed statistically significant PAC (**Figure 2C and D**). Shaded regions indicate standard error over recordings. PAC was estimated for EEG channels FCz and Cz. Grey waves at the top and grey bar at the bottom indicate the phase of the respiratory cycle. Coloured dots indicate points that are statistically significant (alpha level was set to 0.001 with false discovery rate correction). **(B)** Corresponding (uncorrected) statistical significance analogous to the coloured dots at the top of panel A. **(C)** Spatial map of the cross-frequency phase-slope index between respiratory phase ($\omega_{\text{respiratory phase}}$) and EEG amplitude ($\omega_{\text{EEG amplitude}}$) (see **Figure 3—figure supplement 1** for the pan-spectral estimates) and **(D)** its (uncorrected) statistical significance (reported on a logarithmic scale). The spectra show the mean over all recordings. For all panels, data included is from 68 infants (28–42 weeks postmenstrual age [PMA] at time of recording) on 104 recording occasions. See **Table 1** for further clinical and demographic characteristics.

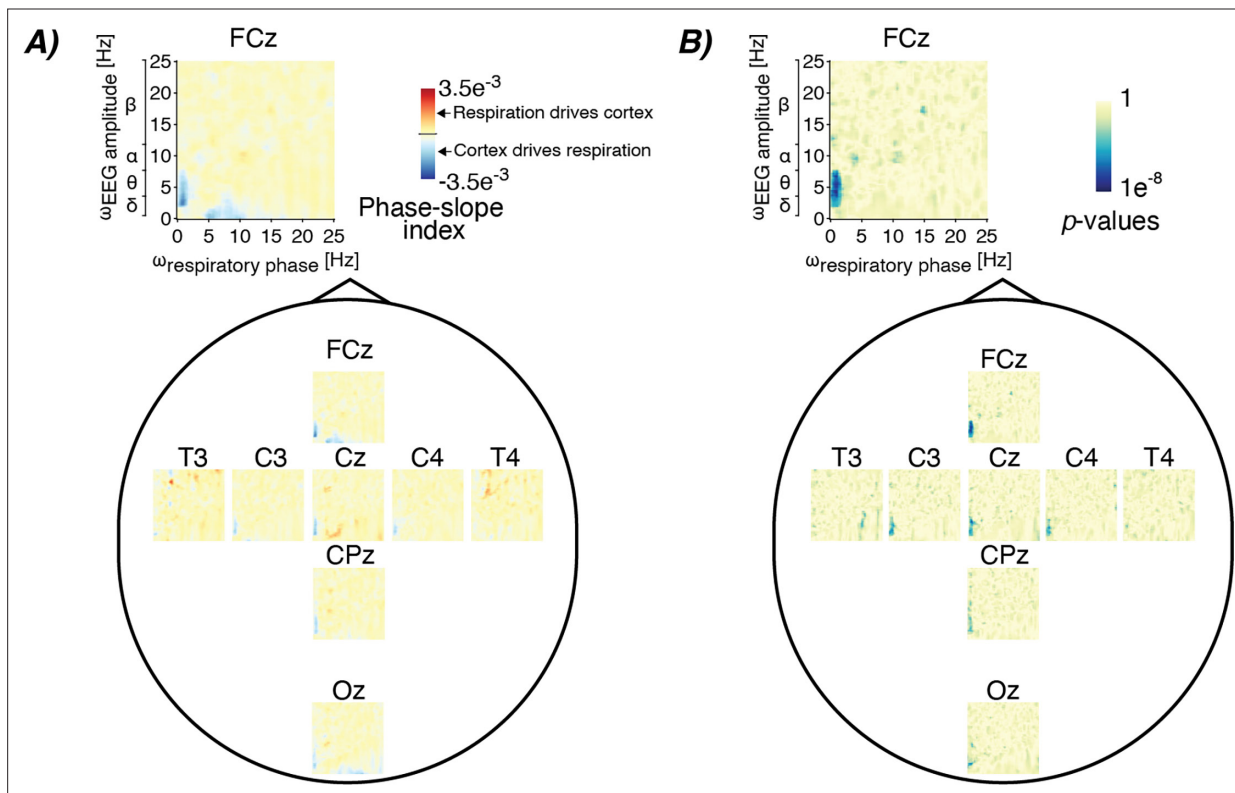


Figure 3—figure supplement 1. Directionality of the cortico-respiratory coupling. **(A)** Spatial map of the phase-slope index between the respiratory phase ($\omega_{\text{respiratory phase}}$) and electroencephalography (EEG) amplitude ($\omega_{\text{EEG amplitude}}$), here shown over full frequency ranges (see **Figure 3** for the zoomed-in spectra). **(B)** The corresponding (uncorrected) statistical significance (reported on a logarithmic scale).

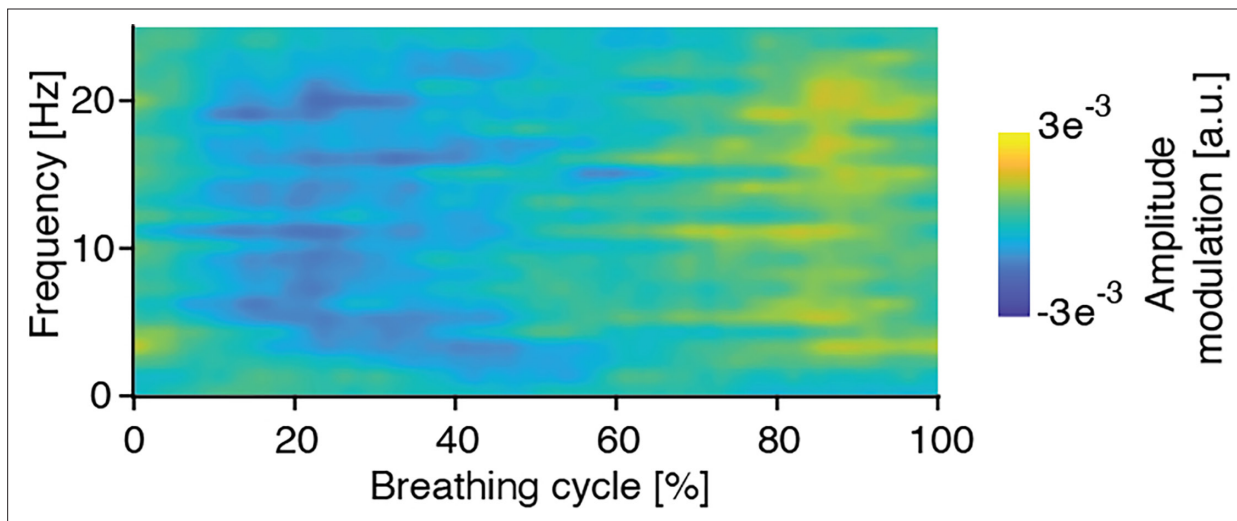


Figure 3—figure supplement 2. Photoplethysmographic amplitude modulation depending on the respiratory cycle and frequency.

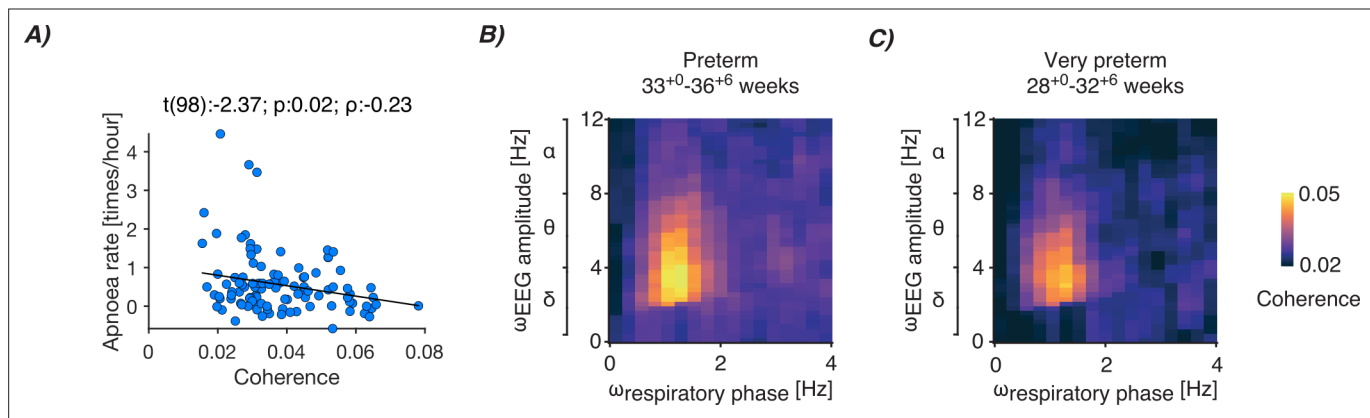


Figure 4. Cortico-respiratory coupling dependency on apnoea rate and postmenstrual age (PMA). **(A)** Relationship between apnoea rate and statistically significant phase-amplitude coupling (PAC; defined as coherence encompassing delta- and theta-band frequencies). Each blue dot is the data of an individual recording (data of 68 infants were included from 104 test occasions). Black linear graph is the best fit of the linear mixed-effects model (fixed factors: coupling averaged over statistically significant samples from channels FCz and Cz [see **Figure 4—figure supplement 1** for channel-specific relationships], data length to determine apnoea rate, mode of ventilation, and PMA; random factor: infant). Panel title contains the test statistic of the predictor's regression slope (t), its significance (p), and partial correlation coefficient (ρ). See **Figure 4—figure supplements 2–4** for data according to PMA and whether or not the infant received caffeine at the time of recording. **(B–C)** PAC spectra between the respiratory phase ($\omega_{\text{respiratory phase}}$) and electroencephalography (EEG) amplitude ($\omega_{\text{EEG amplitude}}$) for **(B)** preterm (58 recordings; 33.0–36.86 weeks) and **(C)** very preterm (28 recordings; 28.0–32.86 weeks) infants. Both spectra are averaged over recordings and EEG channels FCz and Cz.

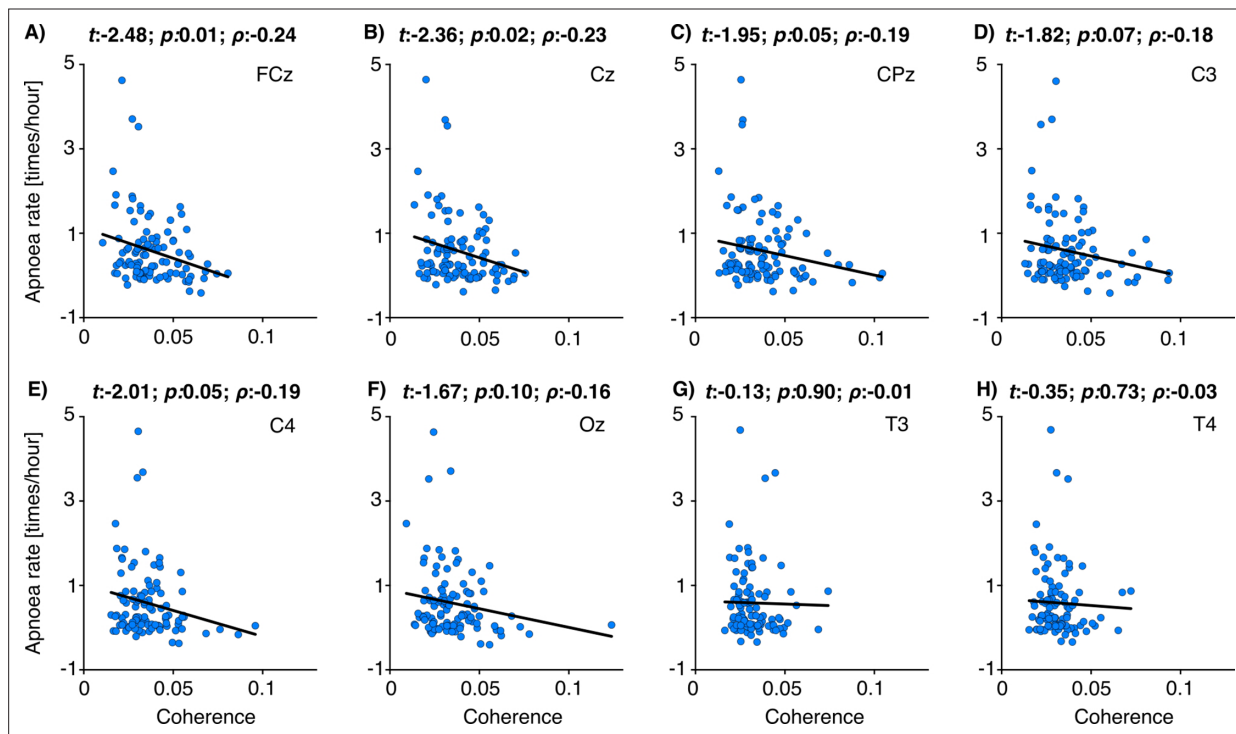


Figure 4—figure supplement 1. Relationships between phase-amplitude coupling and apnoea rate for individual electroencephalography (EEG) channels. Each blue dot is the data of an individual recording (data of 68 infants were included from 104 test occasions). Black linear graphs are the best fit of the linear mixed-effects models (fixed factors: coupling averaged over statistically significant samples at each electrode respectively, data length to determine apnoea rate, mode of ventilation, and postmenstrual age; random factor: infant [random intercept]). Panel titles contain the test statistic of the predictor's regression slope (t), its significance (p), and partial correlation coefficient (ρ). Electrode position is indicated in top right of each panel, with (A) FCz, (B) Cz, (C) CPz, (D) C3, (E) C4, (F) Oz, (G) T3, and (H) T4. Electrodes with weaker coherence overall (see Figure 2C and D) – Oz, T3, T4 – did not show a significant relationship between apnoea rate and coherence as expected as these electrodes do not overlay cortical motor areas.

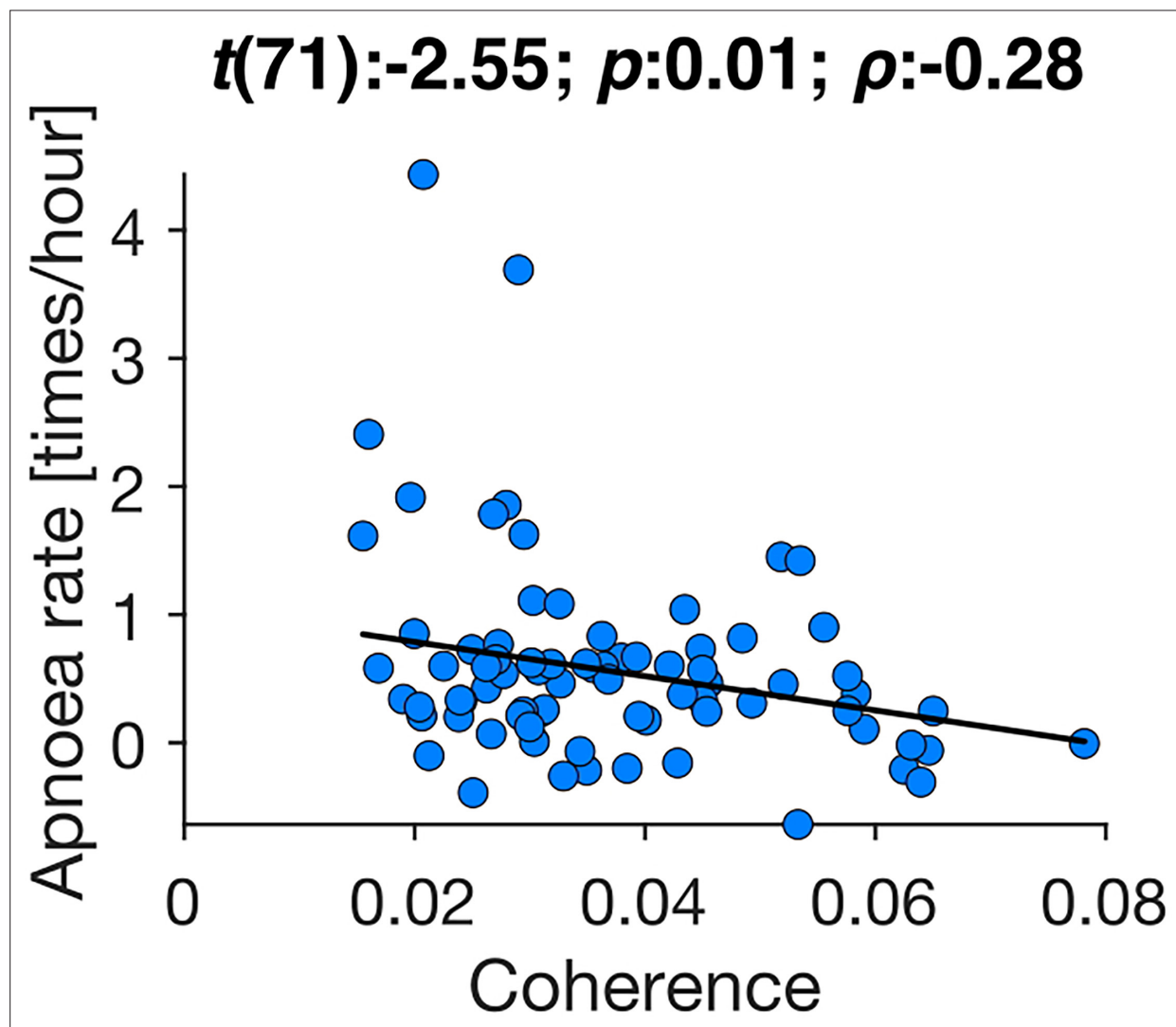


Figure 4—figure supplement 2. Apnoea rate for preterm infants compared with phase-amplitude coupling (PAC) for preterm infants. Relationship between PAC (defined as cross-frequency coherence) and apnoea rate for the preterm infants (≤ 36 weeks postmenstrual age) (data of all infants is presented in **Figure 4**). Each blue dot is the data of an individual recording (data of 53 infants were included from 86 test occasions). Black linear graph is the best fit of the linear mixed-effects model (fixed factors: coupling averaged over statistically significant samples from channels FCz and Cz (see **Figure 4—figure supplement 1** for channel-specific relationships), data length to determine apnoea rate, mode of ventilation, and postmenstrual age; random factor: infant [random intercept]). Panel title contains the test statistic of the predictor's regression slope (t), its significance (p), and partial correlation coefficient (ρ).

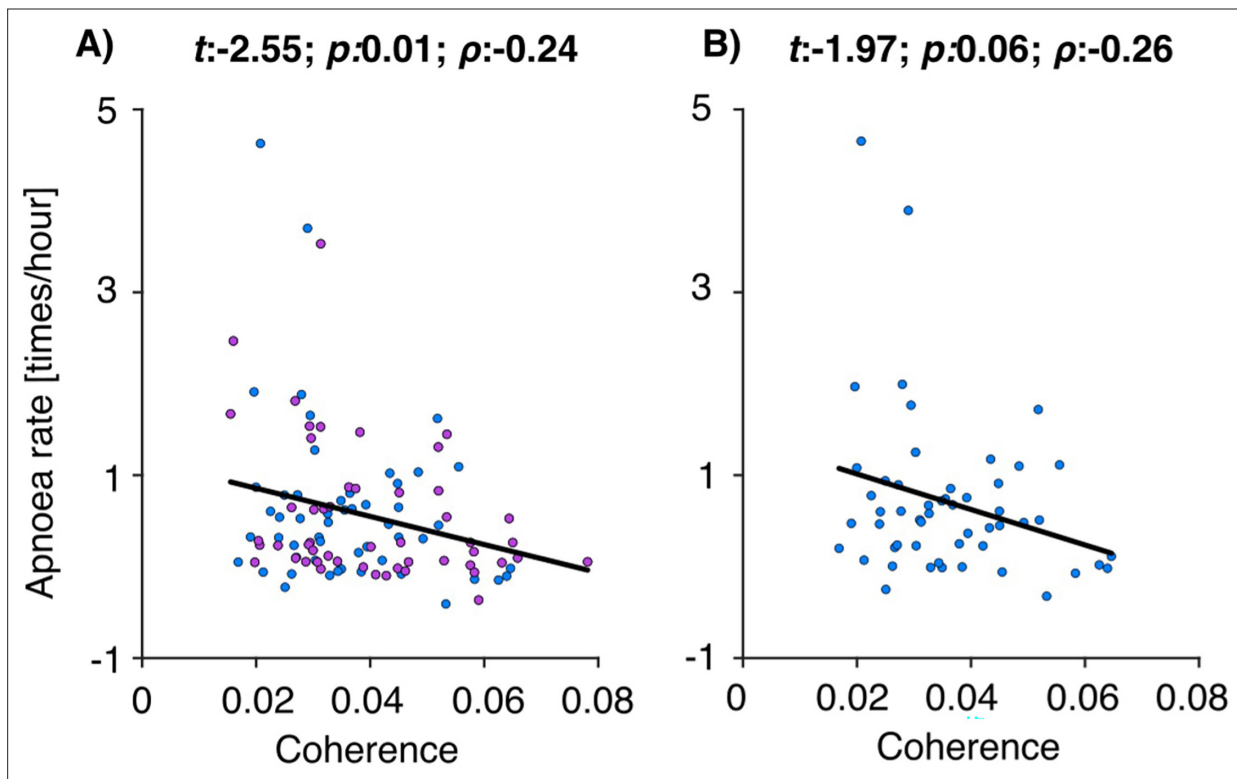


Figure 4—figure supplement 3. Relationship between apnoea rate and phase-amplitude coupling in infants receiving caffeine. **(A)** Data for all recordings, with blue dots indicating sessions where infants had received caffeine (medically prescribed), and purple dots indicate sessions where infants did not have caffeine prescribed on the day of recording (total: 68 infants on 104 recording sessions). **(B)** Stratified analysis for infants receiving caffeine (35 infants on 53 recording sessions). Infants receiving caffeine are more likely to experience apnoeas (which is why caffeine is prescribed). Each dot is the data of an individual recording. Black linear graph is the best fit of the linear mixed-effects model (fixed factors: coupling averaged over statistically significant samples from channels FCz and Cz, data length to determine apnoea rate, mode of ventilation, and postmenstrual age; random factor: infant [random intercept]). Panel title contains the test statistic of the predictor's regression slope (t), its significance (p), and partial correlation coefficient (ρ).

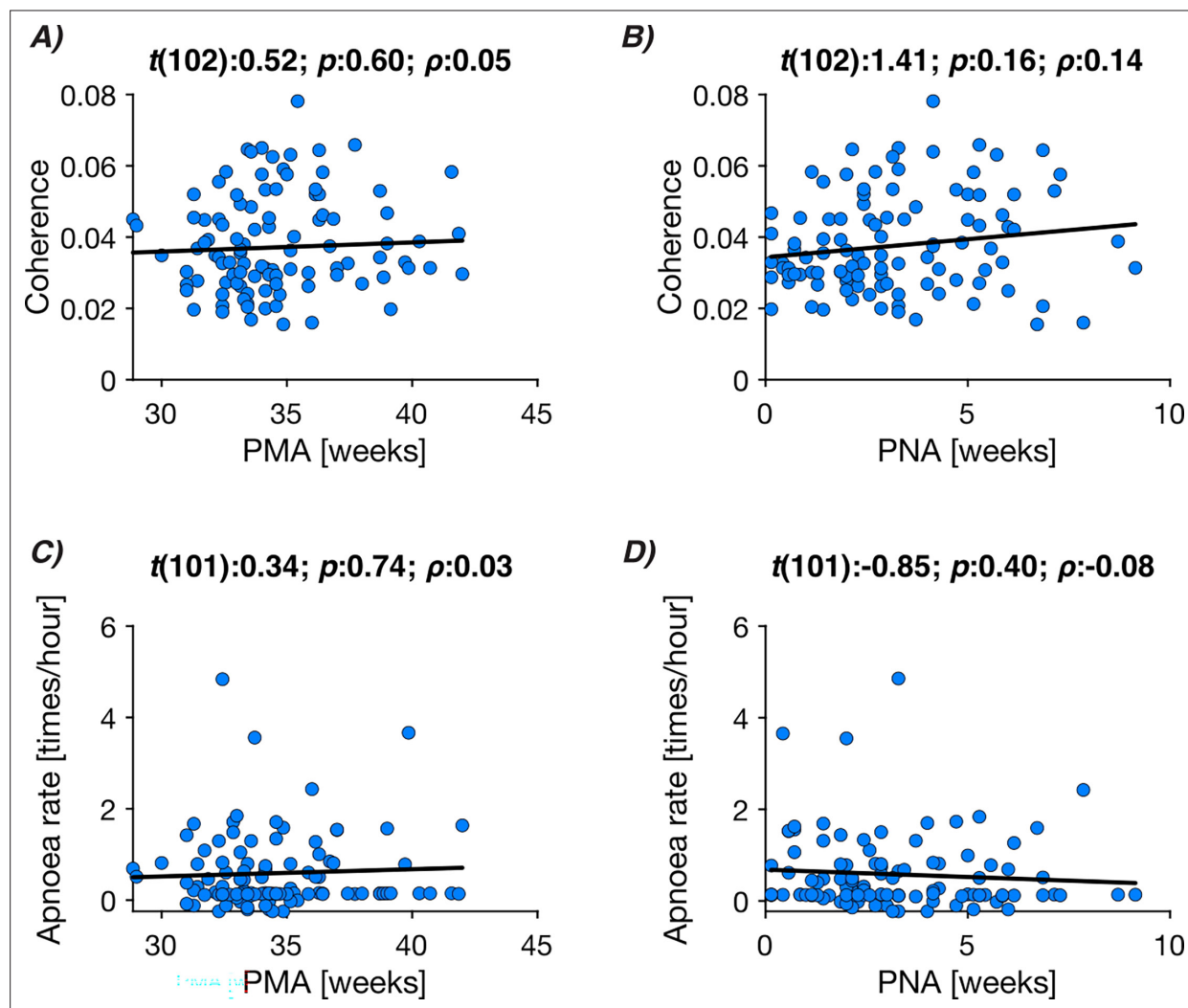


Figure 4—figure supplement 4. Coupling and apnoea rate relationships with age. **(A)** Phase-amplitude coupling (defined as cross-frequency coherence) and **(B)** apnoea rate relationships with postmenstrual age (PMA). **(C–D)** Same relationships over postnatal age (PNA). Each dot is the data of an individual recording (data from 68 infants on 104 test occasions were included). Black linear graphs are the best fit of the linear mixed-effects models (fixed factor: PMA or PNA; random factor: infant – in line with previous publications, the data length of the respiratory signal was additionally included in the models of panels **B** and **D**). Panel titles describe the predictor's test statistic of the regression slope (t), its significance (p), and partial correlation coefficient (ρ).

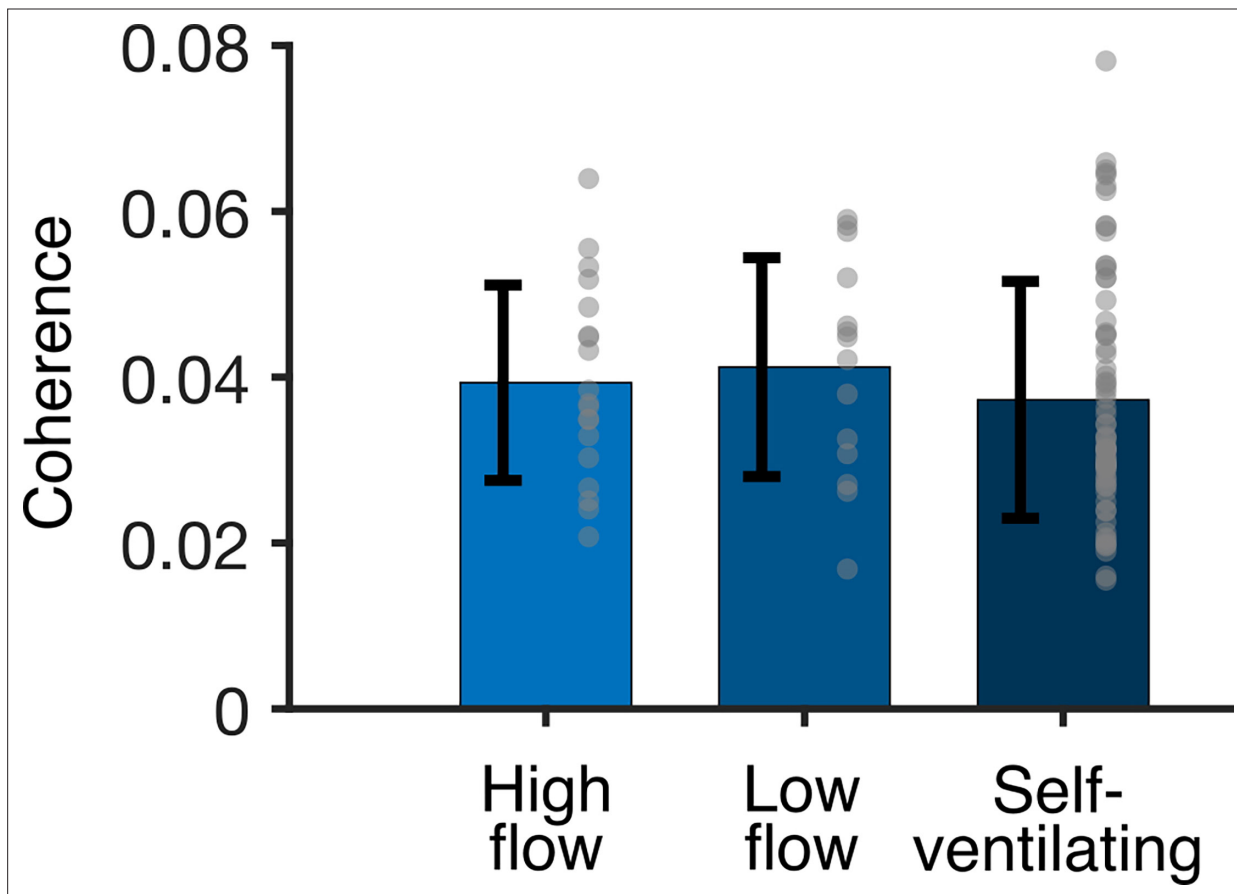


Figure 4—figure supplement 5. Cortico-respiratory coupling as a function of mode of ventilation. Coherence-based phase-amplitude coupling (PAC) were averaged for each recording using the statistical masking obtained from **Figure 2**.